

# An H I absorption distance to the black hole candidate X-ray binary MAXI J1535–571

J. Chauhan<sup>1\*</sup>, J. C. A. Miller-Jones<sup>1</sup>, G. E. Anderson<sup>1</sup>, W. Raja<sup>2</sup>, A. Bahramian<sup>1</sup>, A. Hotan<sup>2</sup>, B. Indermuehle<sup>2</sup>, M. Whiting<sup>2</sup>, J. R. Allison<sup>3</sup>, C. Anderson<sup>2</sup>, J. Bunton<sup>2</sup>, B. Koribalski<sup>2</sup>, E. Mahony<sup>2</sup>

<sup>1</sup>*International Centre for Radio Astronomy Research – Curtin University, GPO Box U1987, Perth, WA 6845, Australia*

<sup>2</sup>*CSIRO Astronomy and Space Science, Australia Telescope National Facility, PO Box 76, Epping NSW 1710, Australia*

<sup>3</sup>*Sub-Dept. of Astrophysics, Department of Physics, University of Oxford, Denys Wilkinson Building, Keble Rd., Oxford, OX1 3RH, UK*

Accepted XXX. Received YYY; in original form ZZZ

## ABSTRACT

With the Australian Square Kilometre Array Pathfinder (ASKAP) we monitored the black hole candidate X-ray binary MAXI J1535–571 over seven epochs from 21 September to 2 October 2017. Using ASKAP observations, we studied the H I absorption spectrum from gas clouds along the line-of-sight and thereby constrained the distance to the source. The maximum negative radial velocities measured from the H I absorption spectra for MAXI J1535–571 and an extragalactic source in the same field of view are  $-69 \pm 4 \text{ km s}^{-1}$  and  $-89 \pm 4 \text{ km s}^{-1}$ , respectively. This rules out the far kinematic distance ( $9.3^{+0.5}_{-0.6} \text{ kpc}$ ), giving a most likely distance of  $4.1^{+0.6}_{-0.5} \text{ kpc}$ , with a strong upper limit of the tangent point at  $6.7^{+0.1}_{-0.2} \text{ kpc}$ . At our preferred distance, the peak unabsorbed luminosity of MAXI J1535–571 was  $> 78$  per cent of the Eddington luminosity, and shows that the soft-to-hard spectral state transition occurred at the very low luminosity of  $1.2 - 3.4 \times 10^{-5}$  times the Eddington luminosity. Finally, this study highlights the capabilities of new wide-field radio telescopes to probe Galactic transient outbursts, by allowing us to observe both a target source and a background comparison source in a single telescope pointing.

**Key words:** black hole physics – ISM: jets and outflows – radio continuum: transients – X-rays: binaries – X-rays: individual: MAXI J1535–571

## 1 INTRODUCTION

Stellar-mass black holes in binary systems play an important role in understanding the universal phenomena of accretion and ejection (Fender, Belloni, & Gallo 2004), as they evolve on humanly observable time-scales. However, black hole X-ray binaries (XRBs) typically have poorly constrained distances, with uncertainties often more than 50% (Jonker & Nelemans 2004). The distance of a stellar object is of great importance as it enables us to determine the physical parameters from observables, such as luminosity from flux, physical separation from angular separation, and velocity from proper motion.

Parallax is the most fundamental and model-independent method for estimating stellar distances. The main caveat of this method is that for typical XRB distances, the measured parallax is extremely small (1 milliarcsec for 1 kpc). Therefore, instruments capable of probing sub-milliarcsecond scales are required. Such studies are possible only with very long baseline interferometry (VLBI) and

*Gaia* (Gaia Collaboration et al. 2018), and only for a handful of XRBs (e.g. Miller-Jones et al. 2009; Reid et al. 2011; Gandhi et al. 2019).

High-precision trigonometric parallax measurements are not possible for most black hole XRBs. In such cases, the distance is commonly estimated by comparing the inferred absolute magnitude of the donor star (as determined from its spectral type) with the apparent magnitude, after considering the maximum contribution from the accretion disk (Jonker & Nelemans 2004). The main limitations of this technique are the uncertainties associated with the disk contribution and the extinction along the line of sight.

If the companion star is too faint (e.g. if the system is highly extinguished) then other methods must be used, one of which uses the Doppler shifted 21-cm absorption line of neutral hydrogen (H I; e.g. Koribalski et al. 1995; Dhawan, Goss, & Rodríguez 2000; Lockman, Blundell, & Goss 2007). Intervening interstellar H I clouds are presumed to follow the rotation of the Milky Way and their absorption features allow us to constrain the kinematic distance to the source (Gathier, Pottasch, & Goss 1986; Kuchar & Bania 1990). If the source is beyond the solar orbit, this method pro-

\* E-mail: j.chauhan@student.curtin.edu.au (JC)

vides an accurate kinematic distance estimation. However, the method suffers from ambiguities if the source lies within the solar orbit (Wenger et al. 2018).

On 2 September 2017, an uncatalogued XRB was co-discovered by the Monitor of All-sky X-ray Image<sup>1</sup> (*MAXI*; Matsuoka et al. 2009) and the Neil Gehrels Swift Observatory (*Swift*; Gehrels, et al. 2004), and designated MAXI J1535–571 (Negoro et al. 2017a; Kennea et al. 2017a). In J2000.0 coordinates, the source is located at RA = 15:35:19.714±0.007, DEC = −57:13:47.583±0.024 (Galactic coordinates  $l=323.72407^\circ$ ,  $b=-1.12887^\circ$ ; Russell et al. 2017a). Multi-wavelength studies of the system strongly suggest that the accreting compact object is a stellar-mass black hole (Dincer 2017; Kennea 2017b; Negoro et al. 2017b; Russell et al. 2017a,b). However, the physical parameters, including the black hole mass and distance, and the peak luminosity of the outburst are still uncertain.

In this study, we aim to constrain the distance to MAXI J1535–571 using H I absorption spectra from Australian Square Kilometre Array Pathfinder (ASKAP) early science observations. ASKAP is a synthesis radio telescope located at the Murchison Radio-astronomy Observatory (MRO) in Western Australia, which has already established its ability to detect H I absorption from extragalactic sources (Allison et al. 2015, 2017). The telescope operates in the frequency range 0.7–1.8 GHz providing an angular resolution of 10 arcsec and a field of view (FOV) of 30 deg<sup>2</sup> at 1.4 GHz (Hotan et al. 2014). This allows us to simultaneously measure the H I absorption towards both MAXI J1535–571 and an extragalactic calibrator source, allowing us to distinguish between near and far kinematic distances.

## 2 OBSERVATIONS AND DATA REDUCTION

During the 2017 outburst of MAXI J1535–571, ASKAP observed the source over seven epochs from 21 September to 2 October 2017. At the time of these early science observations, ASKAP was operated in a sub-array of twelve dishes, which provides an angular resolution of  $\sim 30$  arcsec. All observations were conducted at a central frequency of 1.34 GHz with a processed bandwidth of 192 MHz. The total bandwidth was further divided into 10368 fine channels, each with a frequency resolution of 18.519 kHz, with visibilities recorded every 10 s. Further details of the observations can be seen in Table 1.

We reduced our data using the standard ASKAP data analysis software, *ASKAPsoft*<sup>2</sup> (pipeline version 0.24.1). For continuum imaging, we performed dynamic flagging of faulty antennas, faulty channels, and baselines affected by radio frequency interference (RFI) during bandpass calibration. Bandpass and flux calibration were performed using the calibrator source PKS B1934–638, and the bandpass solution was interpolated across frequencies where data were flagged. The *IMFIT* task in the Common Astronomy Software Application (CASA v5.1.2-4; McMullin et al. 2007) package was used for measuring the flux densities and  $1\sigma$  uncertainties of MAXI J1535–571 from the continuum images, which are listed in Table 1.

With a flux density  $> 150$  mJy during the first four epochs, there was enough signal-to-noise to detect H I absorption towards MAXI J1535–571. We used the *SIMAGER* task to generate spectral-line cubes, and performed only stokes-V flagging to avoid removing the true absorption line in the H I region. We applied the bandpass solutions to the raw spectral data and extracted a sub-spectral cube with 1000 channels centered at 1.42 GHz and a velocity resolution of  $\sim 4$  km/s. Note that our conclusions should not be affected by the Galactic H I absorption towards PKS B1934–638, which is very narrow (FWHM  $< 6$  km/s; approximately one channel wide) and therefore only affects the H I absorption line at local standard of rest (LSR) velocity = 0 km s<sup>−1</sup> (Dénes et al. 2018). We extracted the H I spectra corresponding to MAXI J1535–571 and a nearby extragalactic comparison source PMN J1533–5642 (= MGPS J153358–564218; Griffith & Wright 1993; Murphy et al. 2007), located at RA = 15:33:57.439, DEC = −56:42:17.183 (uncertainty of 10 arcsec), and analysed the H I absorption complexes with significance exceeding  $3\sigma$ .

## 3 RESULTS

The continuum image of the region around MAXI J1535–571 for the 21 September 2017 observation is shown in Figure 1 (left panel), where the source is detected at high significance ( $> 200\sigma$ ). Residual calibration, deconvolution and amplitude errors remain in our images due to these data being obtained during ASKAP’s early science phase with 12 of 36 active antennas, causing reduced UV coverage, the use of the rapidly evolving *ASKAPsoft* software, and the lack of complete instrumental characterisation that will only improve over time. Figure 1 (left panel) also shows the extragalactic comparison source MGPS J153358–564218 with a measured flux density of  $340 \pm 2$  mJy on 21 September 2017, which remained stable to better than 10% between all the epochs.

In the right panel of Figure 1, we present the 1.34 GHz light curve of MAXI J1535–571 from 21 September to 2 October 2017. During this period we observed two distinct peaks on 21 and 23 September, reaching flux densities  $> 450$  mJy, likely corresponding to separate flaring events. Subsequently, the radio flux density of MAXI J1535–571 gradually decreased, reaching a level of  $\sim 20$  mJy by 2 October.

We downloaded the on-demand X-ray light curves from *MAXI* in the energy range 2.0–20.0 keV to create a hardness-intensity diagram (HID) for MAXI J1535–571, presented in Figure 2. From the HID, all our radio observations were taken in the soft-intermediate spectral state (Tao et al. 2018). This confirms that MAXI J1535–571 underwent radio flaring behaviour during the hard-to-soft X-ray spectral state transition, as is typical for XRBs (Fender, Belloni, & Gallo 2004).

### 3.1 H I absorption spectra

In Figure 3, we show the H I spectrum for MAXI J1535–571 for the first epoch (21 September 2017). In the same plot, we also display the spectrum for the extragalactic source MGPS J153358–564218, and the  $3\sigma$  rms noise levels for the spectra of both sources. For both sources, we measured the rms noise per channel from the spectral cube, taking the median noise value in each channel from a number of regions close to the source to mitigate against any faint Galactic H I emission in any given region. The rms noise level for both

<sup>1</sup> <http://maxi.riken.jp/top/index.html>

<sup>2</sup> <http://www.atnf.csiro.au/computing/software/askapsoft/sdp/docs/current/index.html>

**Table 1.** Details of our ASKAP observations of MAXI J1535–571.

Observation ID	Observation Start date (DD-MM-YYYY)	Observation Start time (hh:mm:ss)	MJD <sup>b</sup>	Exposure time (hh:mm:ss)	Flux Density <sup>a</sup> $S_0$ (mJy)	rms noise (mJy beam <sup>-1</sup> )
4340	21-09-2017	03:06:32	58017.17	02:02:26	$579.6 \pm 2.1$	0.74
4364	22-09-2017	01:30:02	58018.12	02:51:50	$156.1 \pm 1.9$	0.72
4367	22-09-2017	10:35:41	58018.50	03:00:56	$306.1 \pm 1.3$	0.54
4374	23-09-2017	13:23:39	58019.58	01:00:52	$478.2 \pm 2.4$	0.91
4410	30-09-2017	03:29:59	58026.23	04:00:56	$39.8 \pm 0.8$	0.53
4414	01-10-2017	03:35:00	58027.23	04:01:01	$26.3 \pm 0.8$	0.54
4418	02-10-2017	03:39:59	58028.24	04:01:22	$21.4 \pm 0.7$	0.52

<sup>a</sup>  $1\sigma$  errors are quoted, calculated by adding in quadrature the  $1\sigma$  error on the Gaussian fit and the  $1\sigma$  rms noise in the image.

<sup>b</sup> Mid point of our observations.

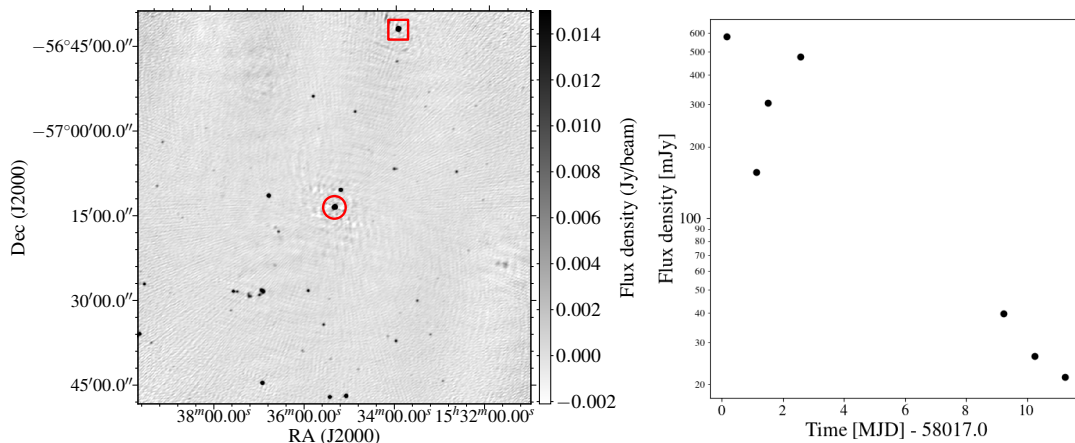


**Figure 1.** Left panel: 1.34 GHz ASKAP continuum image of our 21 September 2017 observation centered at RA = 15:35:19.71, DEC =  $-57:13:47.58$  with a size of  $1.15^\circ \times 1.15^\circ$ . The positions of MAXI J1535–571 and the comparison extragalactic source MGPS J153358–564218 are indicated by the red circle and square, respectively. Right panel: ASKAP light curve of MAXI J1535–571 at 1.34 GHz. The peak flux density of MAXI J1535–571 exceeded 500 mJy.

sources is shown as the dotted line (with their respective red and blue colours) in Figure 3, where  $S_\nu$  is the flux density measured from the data cube and  $S_0$  is that measured from the continuum image via the IMFIT task. In the case of MAXI J1535–571, we observed a significant ( $> 3\sigma$ ) H I absorption complex with a maximum negative velocity of  $-69 \pm 4$  km s<sup>-1</sup>. In the second epoch, the H I absorption lines are weaker due to the lower flux density. Therefore, we have not used the second epoch because the sensitivity was not high enough to reliably determine the maximum velocity out to which absorption could be observed. The third and fourth epochs are excluded from this analysis due to the presence of RFI in the H I spectrum.

For Galactic longitudes  $270^\circ \leq l \leq 360^\circ$ , the expected radial velocities from Galactic rotation are negative. Figure 4 shows the calculated variation of velocity of the local standard of rest ( $V_{\text{LSR}}$ ) with distance from the Sun ( $d$ ) in the direction of MAXI J1535–571. For the determination of  $V_{\text{LSR}}$ , we presumed the Galactic rotation curve to be flat with a circular velocity ( $V_0$ ) and a Galactic centre distance ( $R_0$ ) of  $240 \pm 8$  km s<sup>-1</sup> and  $8.34 \pm 0.16$  kpc, respectively (Reid et al. 2014).  $V_{\text{LSR}}$  is symmetric about the tangent point distance ( $R = R_0 \cos l \equiv 6.7_{-0.2}^{+0.1}$  kpc), and therefore provides two estimates of the distance, near and far, within the solar circle. Beyond  $d = 13.2$  kpc, where  $R > R_0$ ,  $V_{\text{LSR}}$  becomes positive. The kinematic distance to MAXI J1535–571 suffers ambiguities because the source is located within the solar orbit. Furthermore, the gas clouds in the Milky Way may not all be following circular motions. Therefore, we have followed the prescription given by Wenger et al. (2018), who

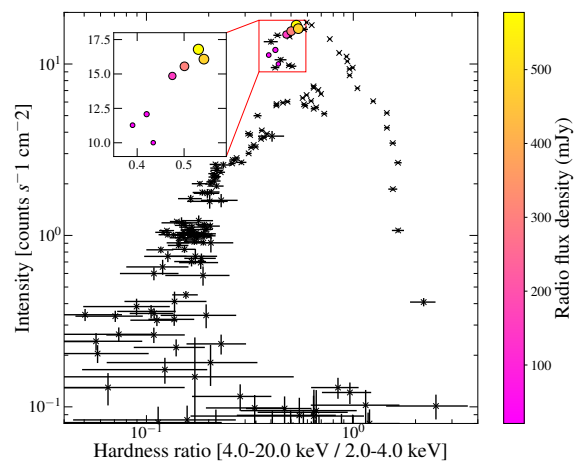


**Figure 2.** Hardness intensity diagram (HID) for the 2017 outburst of MAXI J1535–571. The HID is made from public MAXI data, where intensity is the count rate in the energy range 2.0–20.0 keV, and the hardness ratio is the ratio of count rates in the 4.0–20.0 keV and 2.0–4.0 keV energy bands (Tao et al. 2018). Those X-ray data-points with simultaneous radio detections are highlighted with circles, whose size and color correspond to the measured radio flux density (zoomed in the inset of the plot). The radio flare occurred during the hard-to-soft X-ray spectral state transition.

used the rotation curve given by Reid et al. (2014) with a Monte Carlo approach<sup>3</sup> to derive a more robust kinematic

<sup>3</sup> <http://www.treywenger.com/kd/index.php>

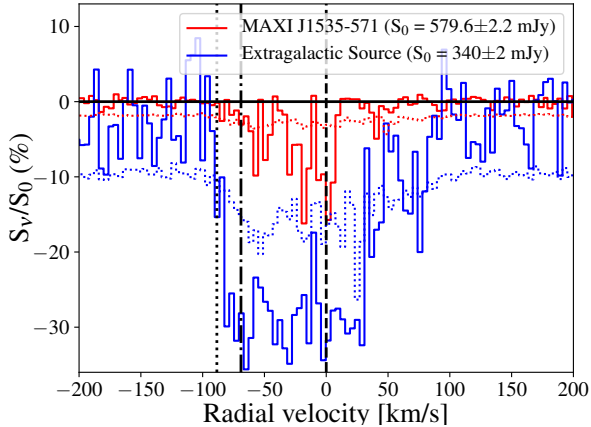


**Figure 3.** The H I absorption spectrum observed from MAXI J1535–571 on 21 September 2017, when the source was brightest ( $S_0 = 579.6 \pm 2.1$  mJy). Spectra of MAXI J1535–571 and the extragalactic source MGPS J153358–564218 (in the local standard of rest frame) are displayed in red and blue, respectively.  $S_\nu$  is measured from the data cube and  $S_0$  is determined from the continuum image. The solid black horizontal line shows the zero flux level. The red and blue dotted lines represent the  $3\sigma$  rms noise levels (calculated directly from individual channel image in the spectral cube) for MAXI J1535–571 and the extragalactic source, respectively. The latter is higher due to being located further out in the primary beam. The dashed vertical line shows the rest velocity. The maximum negative velocity of significant ( $> 3\sigma$ ) absorption in the MAXI J1535–571 spectrum (dash-dotted vertical line at  $-69 \text{ km s}^{-1}$ ) places a lower limit on the source distance of  $4.1^{+0.6}_{-0.5}$  kpc. The maximum negative velocity derived from the extragalactic source spectrum (dotted vertical line at  $-89 \text{ km s}^{-1}$ ) constrains the upper limit on the distance of MAXI J1535–571 to be that of the tangent point at  $6.7^{+0.1}_{-0.2}$

kpc.

distance and uncertainty. Using the observed maximum negative absorption velocity and the methodology of Wenger et al. (2018), we constrain the near and far source distances to be  $4.1^{+0.6}_{-0.5}$  kpc and  $9.3^{+0.5}_{-0.6}$  kpc, respectively.

The H I absorption spectrum of the extragalactic source MGPS J153358–564218 (Figure 3) shows  $> 3\sigma$  significant absorption out to a maximum negative velocity of  $-89 \pm 4 \text{ km s}^{-1}$ , which is due to more distant gas clouds, and consistent (within uncertainties) with the tangent point velocity of  $-92^{+8}_{-9} \text{ km s}^{-1}$  (obtained following Reid et al. 2014 and Wenger et al. 2018). Absorption at the tangent point velocity is not seen towards MAXI J1535–571, implying that MAXI J1535–571 should be located closer than the tangent point distance of  $6.7^{+0.1}_{-0.2}$  kpc (Figure 4).

## 4 DISCUSSION

As outlined in section 3.1, we place a lower limit of  $4.1^{+0.6}_{-0.5}$  kpc on the distance to MAXI J1535–571. The more negative radial velocities detected towards the extragalactic source must therefore be coming from larger distances, out to at least the tangent point at  $6.7^{+0.1}_{-0.2}$  kpc. If we discount the unlikely scenario that all absorption at intermediate velocities comes from gas clouds more distant than the tangent point, we find a most probable distance of  $4.1^{+0.6}_{-0.5}$  kpc for MAXI J1535–571. In the following subsections we discuss the implications of these distance constraints.

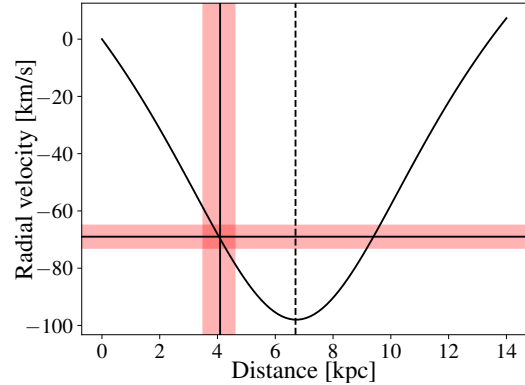


**Figure 4.** The variation of the predicted velocity (for circular rotation) of the local standard of rest ( $V_{\text{LSR}}$ ) as a function of distance from the Sun ( $d$ ), in the direction of MAXI J1535–571. The horizontal line shows the velocity of  $-69 \pm 4 \text{ km s}^{-1}$ , measured from the H I absorption complex of the first epoch. The vertical line displays the most likely distance ( $4.1^{+0.6}_{-0.5}$  kpc) to MAXI J1535–571. The shaded region across both the lines highlight the respective error regions, as derived from the Monte Carlo approach of Wenger et al. (2018). The dashed line displays the position of the tangent point, which is our robust distance upper limit of  $6.7^{+0.1}_{-0.2}$  kpc.

### 4.1 Spectral state transition luminosity

According to Kalemci et al. (2013), the soft-to-hard spectral state transition in black hole XRBs usually occurs between 0.3 and 3 per cent of the Eddington luminosity. A *Swift*/XRT observation on 29 April 2018 was identified as the point of the soft-to-hard spectral state transition (Tao et al. 2018), with an unabsorbed X-ray flux of  $\sim 6 \times 10^{-12} \text{ erg cm}^{-2} \text{ s}^{-1}$ . Using our distance estimates, and assuming a typical black hole mass of  $8 \pm 1 M_\odot$  (Kreidberg et al. 2012), we calculate a transition luminosity of  $1.2 - 3.4 \times 10^{-5}$  times the Eddington luminosity, which is much lower than is typical for black hole XRBs (Kalemci et al. 2013).

Such a peculiar behavior has been seen in a few other sources, and there are a few possible explanations. Vahdat Motlagh, Kalemci, & Maccarone (2019) hypothesised that a new episode of accretion during an outburst decay could launch a new soft state, with a lower transition luminosity than the normal 0.3 – 3 % of the Eddington luminosity. Alternatively, Petrucci et al. (2008) and Begelman & Armitage (2014) suggested that low viscosity or low magnetic fields in the accretion disk could also decrease the state transition luminosity.

### 4.2 Peak X-ray luminosity

Stiele & Kong (2018) observed a peak absorbed X-ray flux of  $\sim 3.7 \times 10^{-7} \text{ erg cm}^{-2} \text{ s}^{-1}$  from MAXI J1535–571 in the energy range 0.6–10 keV. Using our derived distance of  $4.1^{+0.6}_{-0.5}$  kpc, this corresponds to an absorbed luminosity of  $7.5 - 19.9 \times 10^{38} \text{ erg s}^{-1}$ . For a compact object of typical black hole mass  $8 \pm 1 M_\odot$  (Kreidberg et al. 2012), this corresponds to  $> 78$  per cent of the Eddington luminosity. Tao et al. (2018) reported that over the peak of the outburst, the X-ray spectrum could be fit with a slim disk model, suggesting a luminosity close to the Eddington luminosity. Their conclusion is therefore consistent with our distance estimate.

### 4.3 Line-of-sight hydrogen column density

From our distance constraints and Galactic latitude ( $b$ ), we infer MAXI J1535–571 to lie 0.08–0.13 kpc below the Galactic plane, well within the scale height of the Milky Way disk ( $\sim 0.3$  kpc; Mandel 2016). Using X-ray spectroscopy, the absorption column density ( $n_{\text{H}}$ ) towards MAXI J1535–571 was found to be in the range  $2.8 - 5.6 \times 10^{22} \text{ cm}^{-2}$  (Miller et al. 2018; Stiele & Kong 2018; Tao et al. 2018), which is consistent with the predicted Galactic absorption value of  $2.0 \pm 1.0 \times 10^{22} \text{ cm}^{-2}$  in the direction of MAXI J1535–571, calculated from the extinction maps and estimated correlation between  $n_{\text{H}}$  and  $A_{\text{V}}$  (Schlafly & Finkbeiner 2011; Bahramian et al. 2015; Foight, Güver, Özel & Slane 2016).

## 5 SUMMARY

In this study, we measured a kinematic distance to the black hole candidate XRB MAXI J1535–571 using an H I absorption spectrum obtained from ASKAP early science observations. A comparison extragalactic source in the same field shows H I absorption out to  $-89 \pm 4 \text{ km s}^{-1}$  (consistent with coming from the tangent point at  $6.7^{+0.1}_{-0.2}$  kpc), whereas MAXI J1535–571 shows no significant H I absorption beyond  $-69 \pm 4 \text{ km s}^{-1}$ . Therefore, the most probable distance to the source is  $4.1^{+0.6}_{-0.5}$  kpc, with a robust upper limit of  $6.7^{+0.1}_{-0.2}$  kpc.

Our distance constraints have confirmed that MAXI J1535–571 was accreting close to the Eddington rate at the peak of the outburst, in agreement with X-ray spectral fitting results by Tao et al. (2018). We also demonstrate that the soft-to-hard X-ray spectral state transition in MAXI J1535–571 occurred at a very low fraction ( $1.2 - 3.4 \times 10^{-5}$ ) of the Eddington luminosity, which could either be due to a second episode of accretion partway through the outburst decay, or to a low viscosity and magnetic field in the accretion disk.

This study also highlights the importance of modern radio telescopes such as ASKAP, which provide both high sensitivity and a wide field-of-view. In this project, the wide field-of-view of ASKAP afforded us the opportunity to study the H I absorption spectrum of both MAXI J1535–571 and a comparison extragalactic source within the same observation. The high sensitivity and high spectral resolution of ASKAP allowed us to extract the H I spectrum from just two hours of observation, placing stringent constraints on the distance to MAXI J1535–571.

## ACKNOWLEDGEMENTS

We thank the referee for their valuable comments. The Australian SKA Pathfinder is part of the Australia Telescope National Facility which is managed by CSIRO. Operation of ASKAP is funded by the Australian Government with support from the National Collaborative Research Infrastructure Strategy. ASKAP uses the resources of the Pawsey Supercomputing Centre. Establishment of ASKAP, the Murchison Radio-astronomy Observatory and the Pawsey Supercomputing Centre are initiatives of the Australian Government, with support from the Government of Western Australia and the Science and Industry Endowment Fund. We acknowledge the Wajarri Yamatji people as the traditional owners of the Observatory site. JCAM-J is the recipient of Australian Research Council Future Fellowship (project number FT140101082) and GEA is the re-

ipient of an Australian Research Council Discovery Early Career Researcher Award (project number DE180100346) funded by the Australian Government.

## REFERENCES

- Allison J. R., et al., 2015, MNRAS, 453, 1249  
 Allison J. R., et al., 2017, MNRAS, 465, 4450  
 Bahramian A., Heinke C. O., Degenaar N., Chomiuk L., Wijnands R., Strader J., et al., 2015, MNRAS, 452, 3475  
 Begelman M. C., Armitage P. J., 2014, ApJ, 782, L18  
 Dénes H., McClure-Griffiths N. M., Dickey J. M., Dawson J. R., Murray C. E., 2018, MNRAS, 479, 1465  
 Dhawan V., Goss W. M., Rodríguez L. F., 2000, ApJ, 540, 863  
 Dincer T., 2017, ATel1, 10716  
 Fender R. P., Belloni T. M., Gallo E., 2004, MNRAS, 355, 1105  
 Foight D. R., Güver T., Özel F., Slane P. O., 2016, ApJ, 826, 66  
 Gaia Collaboration, et al., 2018, A&A, 616, A1  
 Gandhi P., Rao A., Johnson M. A. C., Paice J. A., Maccarone T. J., 2019, MNRAS, 485, 2642  
 Gathier R., Pottasch S. R., Goss W. M., 1986, A&A, 157, 191  
 Gehrels N., et al., 2004, ApJ, 611, 1005  
 Griffith M. R., Wright A. E., 1993, AJ, 105, 1666  
 Hotan A. W., et al., 2014, PASA, 31, e041  
 Jonker P. G., Nelemans G., 2004, MNRAS, 354, 355  
 Kalemci E., Dincer T., Tomsick J. A., Buxton M. M., Bailyn C. D., Chun Y. Y., 2013, ApJ, 779, 95  
 Kennea J. A., Evans P. A., Beardmore A. P., Krimm H. A., Romano P., et al., 2017a, ATel1, 10700  
 Kennea J. A., 2017b, ATel1, 10731.  
 Koribalski B., Johnston S., Weisberg J. M., Wilson W., 1995, ApJ, 441, 756  
 Kreidberg L., Bailyn C. D., Farr W. M., Kalogera V., 2012, ApJ, 757, 36  
 Kuchar T. A., Bania T. M., 1990, ApJ, 352, 192  
 Lockman F. J., Blundell K. M., Goss W. M., 2007, MNRAS, 381, 881  
 Mandel I., 2016, MNRAS, 456, 578  
 Matsuoka M., et al., 2009, PASJ, 61, 999  
 McMullin J. P., Waters B., Schiebel D., Young W., Golap K., 2007, ASPC, 376, 127  
 Miller J. M., et al., 2018, ApJ, 860, L28  
 Miller-Jones J. C. A., Jonker P. G., Dhawan V., Brisken W., Rupen M. P., Nelemans G., Gallo E., 2009, ApJ, 706, L230  
 Murphy T., Mauch T., Green A., Hunstead R. W., Piestrzynska B., Kels A. P., Sztajer P., 2007, MNRAS, 382, 382  
 Negoro H., et al., 2017a, ATel1, 10699  
 Negoro H., et al., 2017b, ATel1, 10708  
 Petrucci P.-O., Ferreira J., Henri G., Pelletier G., 2008, MNRAS, 385, L88  
 Reid M. J., McClintock J. E., Narayan R., Gou L., Remillard R. A., Orosz J. A., 2011, ApJ, 742, 83  
 Reid M. J., et al., 2014, ApJ, 783, 130  
 Russell T. D., Miller-Jones J. C. A., Sivakoff G. R., Tetarenko A. J., Jacpot Xrb Collaboration, 2017a, ATel1, 10711  
 Russell T. D., Altamirano D., Tetarenko A. J., Sivakoff G. R., et al., Jacpot Xrb Collaboration, 2017b, ATel1, 10899  
 Schlafly E. F., Finkbeiner D. P., 2011, ApJ, 737, 103  
 Stiele H., Kong A. K. H., 2018, ApJ, 868, 71  
 Tao L., et al., 2018, MNRAS, 480, 4443  
 Vahdat Motlagh A., Kalemci E., Maccarone T. J., 2019, MNRAS, 485, 2744  
 Wenger T. V., Balser D. S., Anderson L. D., Bania T. M., 2018, ApJ, 856, 52

This paper has been typeset from a  $\text{\TeX}/\text{\LaTeX}$  file prepared by the author.